

PAPER • OPEN ACCESS

A portable flow tube homogenizer for aerosol mixing in the sub-micrometre and lower micrometre particle size range

To cite this article: Stefan Horender *et al* 2022 *Meas. Sci. Technol.* **33** 114006

View the [article online](#) for updates and enhancements.

You may also like

- [Development of a herbal cream mixer with a homogenizer-stirrer and circulating water cooling system](#)
Suntorn Suttibak, Kamonrat Deesapa, Chayamon Saengmanee et al.
- [Homogenized ion milling over the whole area of EUV spherical multilayer mirrors for reflection phase error correction](#)
T Tsuru, K Arai and T Hatano
- [Homogenization Effect on Nanostructure and Conductivity of Polyaniline Nanofibre Synthesis by Mini-Emulsion Polymerization Technique](#)
M Mohammad, S Kamarudin, N H Mohamed et al.



 **EDINBURGH
INSTRUMENTS**

**NOW WITH MICROPL UPGRADE
FOR SPECTRAL AND TIME-RESOLVED
PHOTOLUMINESCENCE MICROSCOPY.**

edinst.com

A portable flow tube homogenizer for aerosol mixing in the sub-micrometre and lower micrometre particle size range

Stefan Horender¹, Andrea Giordano^{1,2}, Kevin Auderset¹ and Konstantina Vasilatou^{1,*} 

¹ Department of Chemistry, Federal Institute of Metrology METAS, Bern, Switzerland

² Department of Aeronautics, Imperial College London, London, United Kingdom

E-mail: konstantina.vasilatou@metas.ch

Received 25 February 2022, revised 11 July 2022

Accepted for publication 15 July 2022

Published 24 August 2022



CrossMark

Abstract

A portable and light-weight aerosol homogenizer has been designed and validated experimentally. The design relies on large-scale primary standards for particle number and mass concentration previously developed for metrology applications, but the dimensions have been scaled down to produce a versatile and user-friendly apparatus for everyday applications in aerosol sciences. The homogenizer is a 0.8 m long cylinder made of steel with an inner diameter of 50 mm, equipped with three inlets for primary aerosols and up to four outlets for sampling homogenized aerosol mixtures. Mixing is achieved by three turbulent air jets. The aerosol spatial homogeneity in the sampling zone was within $\pm 1\%$ and $\pm 4\%$ for 2 and 5 μm polystyrene (PS) particles, respectively. The possibility to supply and control independently aerosol flows with pressure-sensitive generators and the short equilibration time (<1 min) have also been demonstrated. The homogenizer allows for mixing various aerosol components, such as soot, inorganic species and mineral dust particles, to generate ambient-like aerosols in the laboratory or industrially manufactured particles such as PS spheres as model aerosols. We believe that it could have applications in applied aerosol research, health-related studies, and instrument calibration.

Keywords: flow, tube, homogenizer, aerosol, mixing, micrometre particles, calibration

(Some figures may appear in colour only in the online journal)

1. Introduction

Airborne particulate pollutants contribute to climate change and have been linked to adverse health effects (Loomis *et al* 2013, WHO 2013, Fuzzi *et al* 2015, Kim *et al* 2015). Exposure to elevated levels of particulate matter (PM) can decrease

life expectancy by up to 36 months, thus contributing to hundred of thousands of premature deaths per year in Europe alone (Fuzzi *et al* 2015). For EU member states, air quality monitoring is mandatory and comprises quantification of airborne PM and some of its constituents (European Parliament 2008). Similar regulations exist in the USA, Switzerland and many other countries.

Ambient PM is a highly complex mixture, including combustion particles, inorganic species, mineral dust, primary and secondary organic matter, bioaerosols and other materials (Harrison 2020). Moreover, the physicochemical properties of ambient aerosols vary considerably by location and by time of day and season, depending on local emission sources and climate conditions. Calibration/characterization

* Author to whom any correspondence should be addressed.



Original content from this work may be used under the terms of the [Creative Commons Attribution 4.0 licence](https://creativecommons.org/licenses/by/4.0/). Any further distribution of this work must maintain attribution to the author(s) and the title of the work, journal citation and DOI.

of aerosol monitoring instruments is often performed outdoors with lengthy and expensive field campaigns. However, since the PM composition of ambient air is neither stable nor exactly known, these experiments cannot be reproduced.

To reduce the labour time and costs required for instrument calibration, controlled laboratory-based procedures have been proposed in the past. For instance, calibration of PM monitors, reporting aerosol mass concentration ($\mu\text{g m}^{-3}$) of selected size fractions, can be performed starting with simple model aerosols, e.g. with dust, salt particles or mixtures thereof (Hoge *et al* 2004, Schwab *et al* 2004, Liu *et al* 2017, Papapostolou *et al* 2017) or with more complex ambient-like aerosols (Horender *et al* 2021a). For homogenizing aerosols, large-scale aerosol mixing chambers with a volume of 1.3 m^3 (Papapostolou *et al* 2017) and flow tube homogenizers of 100–350 l have been reported in the literature (Hoge *et al* 2004, Schwab *et al* 2004, Liu *et al* 2017, Horender *et al* 2021a, 2021b).

Similarly, for the calibration of optical particle size spectrometers (OPSSs), according to the ISO 21501-1 standard (ISO 21501-1 2009) the use of an aerosol mixing chamber (also known as a distribution chamber) is recommended for mixing polystyrene (PS) particles and delivering these in parallel to the OPSS under test and the reference particle counter. Again, large-scale flow tube homogenizers have been described in the literature (Horender *et al* 2019), which are ideal for applications in metrology, but cannot be easily operated or replicated by industry or other calibration laboratories.

For the calibration of bioaerosol instruments, different aerosol mixing chambers have been reported (see Pogner *et al* 2019 and references therein), but particle concentrations often depend on the relative position within the box-shaped chamber (Wong *et al* 2010), with overall variations of up to 37% between the different positions (Konlechner *et al* 2013).

The goal of this study was to design a flow tube homogenizer that is portable and user friendly and still allows for a high aerosol spatial homogeneity for particles in the lower micrometre range. A portable flow tube homogenizer with a total height of $\sim 0.8\text{ m}$ and an inner tube diameter of 50 mm (i.e. volume of $\sim 8\text{ l}$) was built and experimentally validated. Despite the small dimensions, an aerosol spatial homogeneity within 4% (coverage factor $k = 2$; 95% confidence level) in number concentration at four different sampling ports can be achieved for $5\text{ }\mu\text{m}$ PS particles.

We believe that the portable homogenizer reported in this study can be applied in the calibration of common aerosol instruments, such as portable PM monitors, OPSS, and bioaerosol particle counters. Furthermore, it can serve as a useful tool for basic research and health-related studies whenever mixing of laboratory-generated model aerosols is required.

2. Results and discussion

2.1. Design of portable flow tube homogenizer

A computer-aided design (CAD, Inventor Professional 2019, Autodesk, USA) of the portable aerosol flow tube homogenizer is shown in figure 1. The homogenizer is a custom-made

cylindrical stainless steel tube, oriented vertically, with an inner diameter of 50 mm. As illustrated in figure 1(a), three versions of the homogenizer were built, with a distance d between the aerosol injection point and sampling probes of 75, 57 and 35 cm, respectively. The tube is equipped with three identical inlets for the injection of primary aerosols, which are placed at the very top, as shown in figures 2(b) and (c) (marked in yellow). Since the distance between the inlets is much larger than their inner pipe diameter, no considerable agglomeration (internal mixing) of the injected aerosols is expected. Dilution air (filtered, humidity and temperature controlled) is delivered through seven additional inlets at a total flow rate of $20\text{--}40\text{ l min}^{-1}$ (marked in green in figure 1(b)). The dilution air sweeps the particles down the tube, where they are further mixed by three turbulent air jets (total flow rate of $10\text{--}20\text{ l min}^{-1}$). The three air-jet injection tubes are placed symmetrically around the homogenizer tube (figure 2(c)). Note that the design of the aerosol and air-jet inlets has been modified compared to previous studies (Horender *et al* 2019, 2021a) to facilitate easier construction and maintenance. The total flow rate of the homogenized aerosol is equal to $30\text{--}60\text{ l min}^{-1}$ plus the flows of the primary aerosols. The temperature and relative humidity of dilution and mixing air can be adjusted as described in (Horender *et al* 2021a). The setup can accommodate up to four sampling ports at the bottom of the tube, right above the aerosol exhaust, which will be presented in section 3.

2.2. Experimental validation of aerosol homogeneity

To characterize the aerosol spatial homogeneity in the flow tube as a function of particle size, sodium chloride (NaCl) and PS particles with a geometric mean mobility diameter (GMD_{mob}) of $\sim 0.1\text{ }\mu\text{m}$ and nominal geometric diameter of $2\text{--}5\text{ }\mu\text{m}$, respectively, were generated using a nebulizer (AKG2000, Palas Germany). When nebulizing PS suspensions, residue particles were filtered out with an aerodynamic aerosol classifier (AAC, Cambustion, UK).

Two parallel sampling lines were inserted into the flow tube. The position of the first sampling line was kept fixed at the centre ($i = 0\text{ mm}$), whereas the other one was placed consecutively at a distance $i = -17\text{ mm}$, -9 mm , $+9\text{ mm}$ and $+17\text{ mm}$ with respect to the centre. For each experimental series, eight measurements were carried out, with four measurements along each axis of the sampling cross section. The outlet of each sampling line was connected to a calibrated CPC (Model 5.412, Grimm GmbH, Germany and Model 3775, TSI Inc., USA). During the data analysis, the particle number concentration measured at the sampling line located at the centre was used as reference (C_{ref}). Aerosol spatial homogeneity, η_{hom} , was calculated as the arithmetic average of C_i/C_{ref} , with C_i and C_{ref} the number concentrations measured at the radial positions i (-17 mm , -9 mm , 9 mm , 17 mm) and zero, respectively.

In a first step, three series of experiments were carried out as summarized in table 1. The parameters varied were the particle diameter, the length of the homogenizer and the flow rates of dilution and mixing air. The aerosol spatial homogeneity,

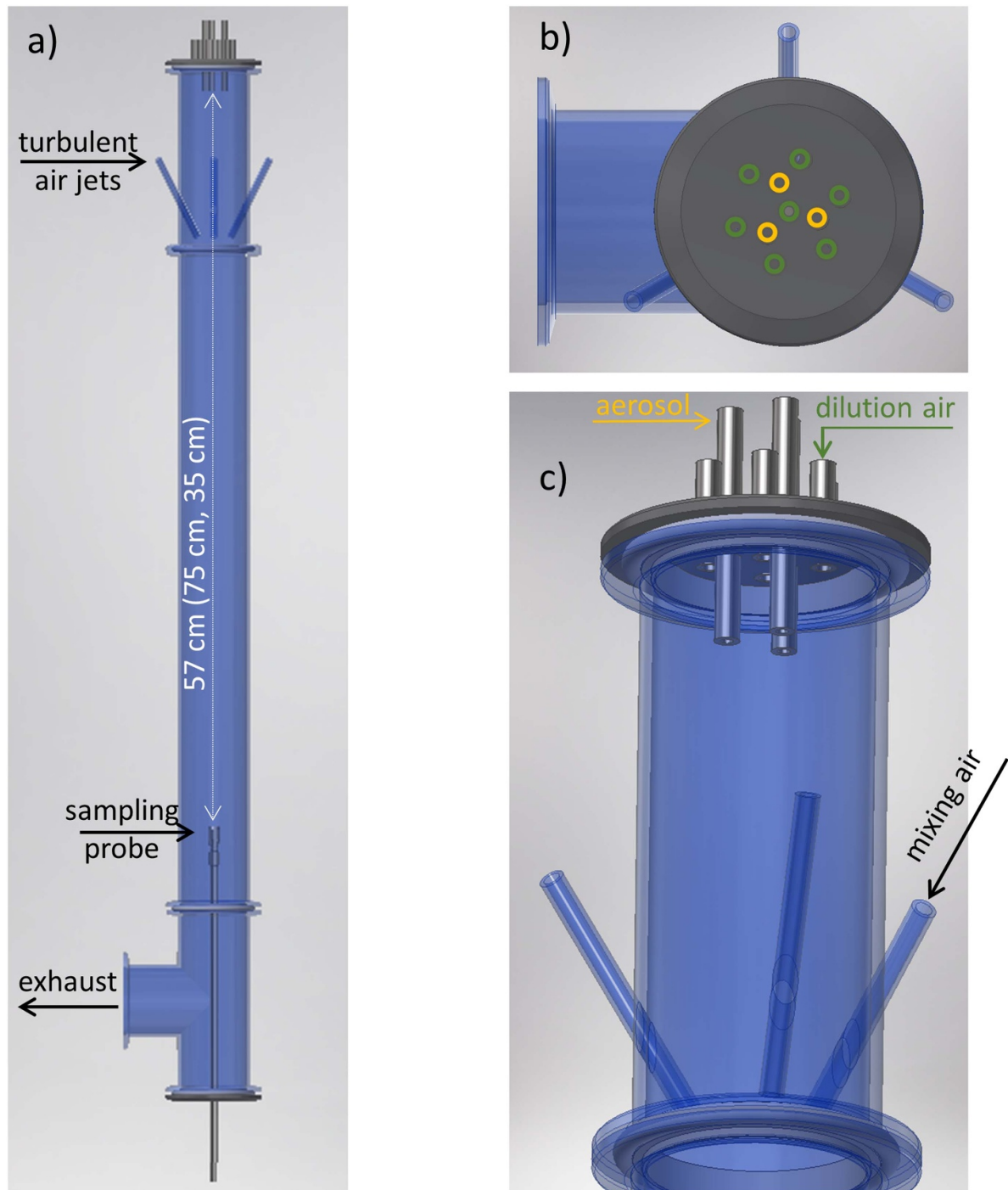


Figure 1. (a) CAD of the aerosol flow tube homogenizer. The distance between the aerosol injection point and the sampling probe d is 57 cm, but configurations with distances of 75 and 35 cm were also tested (see text for more details). For simplicity, only one sampling probe is shown. Panel (b) shows a top-view image of the setup. The three aerosol inlets are marked in yellow and the seven inlets for dilution air are marked in green. Panel (c) shows an enlarged view of the upper part of the setup with the inlets for the primary aerosols, dilution air and mixing air. All components are made of stainless steel. The flow tube homogenizer and the inlets for mixing air are illustrated as transparent for visualization purposes only.

η_{hom} , was found to be 1 (or very close to 1) with the exception of series 3, where η_{hom} decreased to about 0.95, thus indicating an elevated particle number concentration in the centre of the homogenizer. The expanded relative uncertainty U_{rel} (coverage factor $k = 2$; 95% confidence level) of η_{hom} listed in table 1

corresponds to the maximum absolute deviation of the ratio C_i/C_{ref} from 1.

At such small particle sizes ($\text{GMD}_{\text{mob}} \leq 100$ nm, series 1–3), the aerosol was found to be homogeneous within $<0.5\%$ – 1% in number concentration even when the distance d

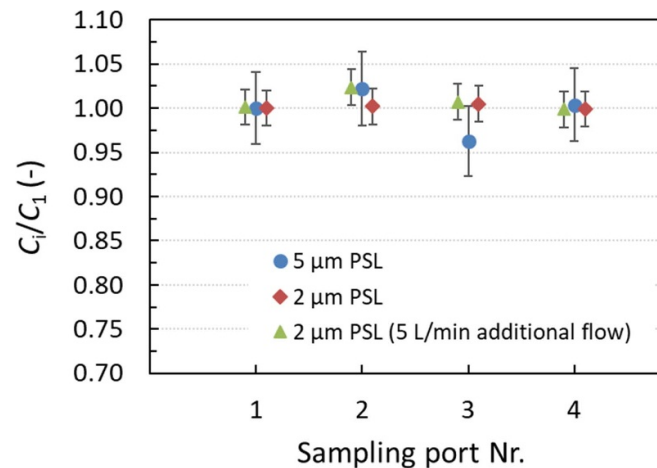


Figure 2. Sampling port bias for (a) 2 and 5 μm PS particles, and (b) for 2 μm PS particles with an additional air flow of 5 l min^{-1} through a second inlet. Error bars designate calculated uncertainties ($k = 2$) due to the random particle distribution (i.e. calculated based on Poisson statistics).

Table 1. Summary of aerosol spatial homogeneity measurements and experimental conditions.

Series	Aerosol type	Geometric mean mobility diameter (μm)	Distance d between aerosol injection and sampling (cm)	Expanded relative uncertainty of $\eta_{\text{hom}} U_{\text{rel}}$ ($k = 2$; 95% confidence level)		
				Dilution-air-to-mixing-air flow rate: 40/20	Dilution-air-to-mixing-air flow rate: 20/10	Dilution-air-to-mixing-air flow rate: 10/10
1	NaCl	~ 0.1	75	0.5%	1%	2%
2	NaCl	~ 0.1	57	0.5%	1%	1%
3	NaCl	~ 0.1	35	3%	4%	6%

between the aerosol injection and sampling point was reduced from 75 to 57 cm. Reducing the dilution-air and mixing-air flow rate down to 10 l min^{-1} did not significantly compromise the aerosol mixing properties. Conversely, when d was reduced to 35 cm, η_{hom} dropped to about 0.95 and U_{rel} increased to 3% for a dilution-air-to-mixing-air flow rate of 40/20 and up to 6% for a dilution-air-to-mixing-air flow rate of 10/10. It should be noted that even at the lowest flow rate, 10/10, the flow is turbulent since the flow structure in the main pipe is a direct consequence of the flow in the inlets, which is turbulent. The only effect of the local Reynolds number is the relaminarization of the flow. However, this process is not at all immediate: the flow needs to run a few diameters before returning laminar even for pipe Reynolds numbers as low as 500 (we refer the reader to Giordano 2020, Horender *et al* 2019 for a detailed discussion on turbulence effects).

The measurements listed in table 1 indicate, as expected, that the longer the tube length and higher the flow rates (Reynolds number approximately 1800 for the 40/20 configuration), the better the aerosol spatial homogenization at the sampling location. Based on these measurements, we decided to fix the distance d to 57 cm and the dilution-air-to-mixing-air flow rate to 40/20.

In a second step, we equipped the setup with isokinetic sampling probes (figure 1(b)). Due to the small inner diameter

(50 mm) of the portable homogenizer, only a maximum of four isokinetic sampling probes for instruments with an aerosol flow of $\leq 3 \text{ l min}^{-1}$ can be accommodated, as shown in figure 1(c). The inner diameter of each sampling cone was 10 mm, the outer diameter 12 mm and the distance between the cones 2 mm (figure 1(d)). Even though the setup is symmetric, the ports were numbered 1–4 for quality assurance.

To experimentally test and characterize the sampling bias between the four probes, the concentration of the aerosol extracted through these ports was compared pairwise using two particle counters. One particle counter was connected to port number 1, while the second counter was successively connected to port numbers 2, 3 and 4. Experiments with two different particle sizes were performed, as described below.

(a) The 2 μm PS particles were dispersed with a glass nebulizer (Type K1, Meinhard, USA), size-selected by an Aerodynamic Aerosol Classifier (AAC, Cambustion Ltd, UK) and measured with a Grimm 11-D (GRIMM GmbH, Germany; sampling flow 1.2 l min^{-1}) and an AeroTrak (TSI Inc., USA; sampling flow 2.7 l min^{-1}). The aerosol number concentration was $\sim 3.5 \text{ cm}^{-3}$ and each measurement lasted 4 min. To investigate whether simultaneous injection of air through another aerosol port would have an effect on the particle homogeneity, the experiment was

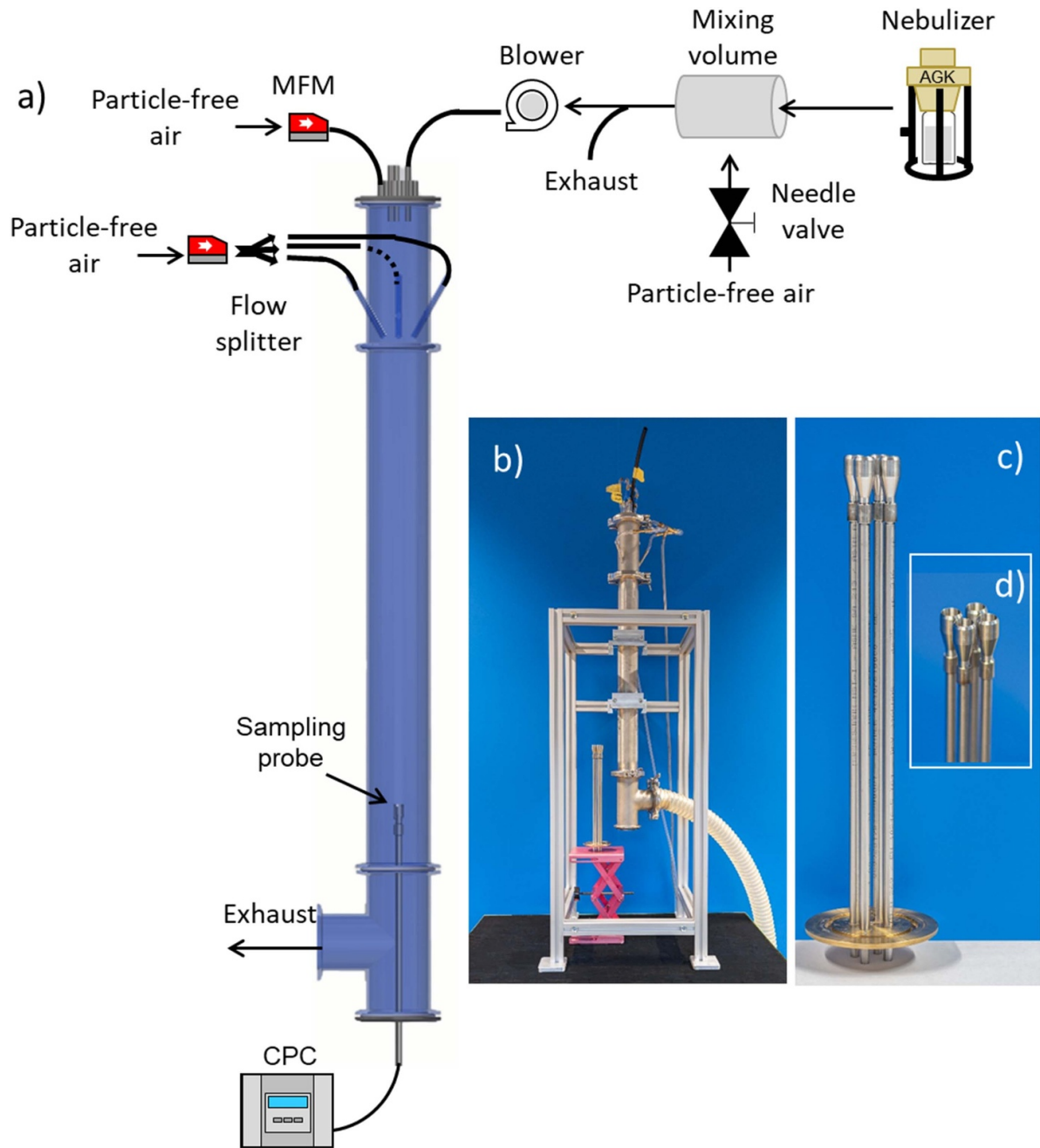


Figure 3. (a) Schematic illustration of the setup used to demonstrate that the aerosol mixing process is independent from the pressure in the flow tube. (b) Picture of the flow tube homogenizer; (c) and (d) close-up view of the four isokinetic sampling ports used for the experiments described in sections 2.2–2.4.

repeated with 5 l min^{-1} particle-free air supplied through a second inlet.

- (b) The $5 \mu\text{m}$ PS particles were dispersed with the Meinhard nebulizer and measured without size selection with two Grimm 11-D OPSS. The aerosol number concentration was $\sim 1.1 \text{ cm}^{-3}$ and each measurement lasted 2 min.

Through each of the two unused ports, 1.2 l min^{-1} were extracted with a pump so that the setup is symmetric. The results are presented in figure 3. It can be seen that for PS particles with geometric diameter $d_{\text{PSL}} = 2 \mu\text{m}$, the measured port bias

in number concentration is within $\pm 1\%$ (red diamonds), while for the $5 \mu\text{m}$ PS particles, it lies within $\pm 4\%$ (blue spheres). Moreover, the simultaneous air supply of 5 l min^{-1} through a second aerosol inlet had hardly any effect on the aerosol homogeneity (green triangles). With $\eta_{\text{hom}} \approx 1$ and an expanded relative uncertainty U_{rel} of $\leq 4\%$, the portable homogenizer performs almost as well as the larger flow tube homogenizers presented in previous studies (Horender *et al* 2019, 2021a). Table 2 provides a comparison of different flow tube homogenizers in terms of dimensions, flow profile and aerosol mixing characteristics.

Table 2. Comparison of different flow tube homogenizers in terms of dimensions, flow profile and aerosol mixing characteristics for particles with geometric diameters in the lower micrometre range (up to about 5 μm). U_{rel} designates the maximum deviation of the measured aerosol homogeneity from the value 1.

Aerosol homogenizer	Total length (m)	Inner diameter (mm)	Total dilution and mixing air flow (l min^{-1})	Flow profile at the sampling region	Reynolds number	Particle velocity (m s^{-1})	U_{rel} (95% confidence level)
(Horender <i>et al</i> 2019)	4	164	180	Turbulent	1800	~ 0.2	1.1%
PALMA (Horender <i>et al</i> 2021a)	2.1	164	180	Turbulent	1800	~ 0.2	2.6%
This study	~ 0.8	50	60	Turbulent	1800	$\sim 0.6^{\text{a}}$	1% ($d_{\text{PSL}} \leq 2 \mu\text{m}$); 4% ($d_{\text{PSL}} = 5 \mu\text{m}$)

^a For total aerosol flow rate up to about 10 l min^{-1} .

Table 3. Results of the experiment demonstrating the pressure independence of the aerosol supply.

Additional flow (l min^{-1})	Total flow ^a (l min^{-1})	Normalized dilution factor	Calculated NaCl particle number concentration (cm^{-3})	Measured NaCl particle number concentration (cm^{-3})	Deviation between measured and calculated concentration (%)
0	60	1	10 400	10 400	—
6	66	1.1	9455	9600	1.5
12	72	1.2	8667	8700	0.4

^a The flow of NaCl aerosol (0.26 l min^{-1}) is negligible.

The setup presented in figures 1 and 3(b) is suitable for the majority of portable PM monitors and OPSS, which indeed have a sample flow rate below 3 l min^{-1} (Vasilatou *et al* 2021). This is also the case for certain bioaerosol monitors, such as the Rapid-E (when operated without a concentrator; Plair, Switzerland) and the WBS-NEO (DMT, USA) (Šauliene *et al* 2019, Lieberherr *et al* 2021). However, for optical particle counters with a sampling flow of 28.3 l min^{-1} and bioaerosol monitors equipped with a concentrator, such as the Poleno (Swisens, Switzerland) and Biotrak (TSI Inc., USA), which run at much higher flow rates (40 and 28.3 l min^{-1} respectively), only one isokinetic sampling probe will fit into the portable homogenizer (Sauvageat *et al* 2020).

2.3. Demonstration of (pressure) independence of aerosol injection

Apart from the small dimensions, the flow tube homogenizer has the advantage that the pressure inside the tube is nearly independent from the aerosol flow rate delivered at each of the three aerosol inlets. In other words, the flow of each aerosol injected into the flow tube can be varied independently without affecting the aerosol mixing characteristics. Validation was performed with the setup shown in figure 1(a). Sodium chloride (NaCl) particles were nebulized with an AGK Generator (Palas, Germany) and were diluted with pressurized particle-free air in a small mixing volume. A blower (model H015X-525A9 with controller, Micronel AG,

Switzerland) transferred a small amount of this aerosol into the tube homogenizer through a 2.5 m long flexible Tygon[®] silicone tube (6 mm inner diameter) at a flow rate of 0.26 l min^{-1} (measured with a Gilibrator-2, Sensidyne, USA). Note that when the pipe was extended to 5.5 m , the flow rate dropped to 0.13 l min^{-1} , showing that the delivered flow rate of the blower is very sensitive to back pressure. The homogenizer was operated at the standard $40/20 \text{ l min}^{-1}$ flow rates as described earlier. Additional particle-free pressurized air was supplied at $0, 6$ and 12 l min^{-1} to the homogenizer through a second aerosol inlet and the aerosol number concentration was monitored with a condensation particle counter (model 5.403, Grimm, Germany) connected to a (single) sampling probe, as shown in figure 1(a). The measured aerosol concentrations are presented in table 3.

The percent deviation between the measured NaCl particle number concentration and the calculated one (based on the dilution relative to 0 l min^{-1} additional flow) is very small, around 1%, although an additional flow larger than the NaCl aerosol flow by at least 1 order of magnitude was delivered to the homogenizer through a separate aerosol inlet. This indicates that the NaCl aerosol flow delivered by the blower is not influenced by any additional aerosol flow injected into the homogenizer, even though the operation of blowers, is known to be very sensitive to changes in back-pressure. It can be concluded that this tube homogenizer allows for the control and mixing of several aerosol flows in a simple manner, without any interference between the different aerosol inlet ports.

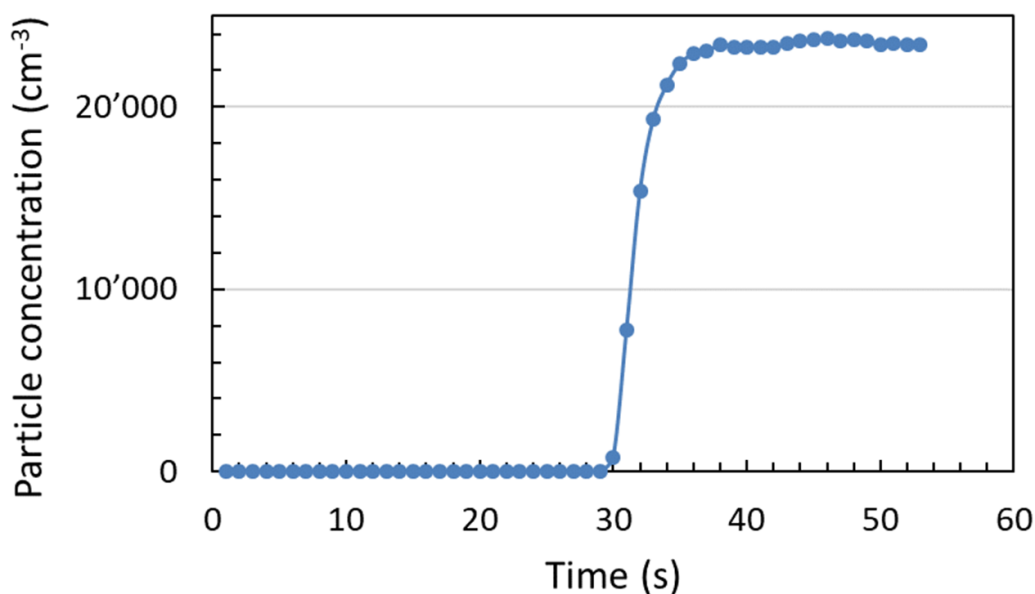


Figure 4. Equilibration time of PS particles with nominal diameter of 900 nm.

2.4. Equilibration time of aerosol mixing

Performing experiments with different aerosol mixtures and concentrations can be very time-consuming with fan-stirred chambers since the whole volume of, typically, several hundred litres has to be exchanged by the aerosol inflows, which are usually only at rates of up to several tens of litres per minute. For the current design, the concentration and mixture of an aerosol can be adjusted very quickly and it takes only a few seconds to equilibrate. An example is shown in figure 4. The particle concentration was measured with a CPC at one of the sampling ports, and the aerosol (PS particles with nominal diameter of 900 nm) was switched on at around 27 s. It can be seen that the measured aerosol concentration equilibrates after approximately 10 s. However, the drawback of the current design is that it cannot achieve very high aerosol concentrations.

3. Summary and conclusions

A portable aerosol homogenizer has been designed and validated experimentally. The homogenizer is a 0.8 m long cylindrical tube made of steel with an inner diameter of 50 mm. It is equipped with three inlets for primary aerosols, which allow nearly independent flow injection, and up to four outlets for sampling the homogenized aerosol mixture. The total flow rate is about 60 l min^{-1} and the aerosol spatial homogeneity in the sampling zone was found to be within 4% in particle number concentration for $5 \mu\text{m}$ sized PS particles. For homogenizing aerosols in the sub-micrometre range, the total length of the tube can be further reduced to 0.6 m. Moreover, the possibility to independently supply and control aerosol flows from pressure-sensitive generators and the short (<1 min) equilibration time have been demonstrated. The

homogenizer is portable, can easily be standardized and replicated, and can even fit into a laboratory fume hood when working with toxic gases and aerosols. We believe that it offers a useful alternative to large-scale mixing chambers whenever maximum ease of use and low operation costs are required, e.g. for instrument calibration against a reference standard by the manufacturer or other accredited laboratories. Furthermore, it can serve as a useful tool for basic research and health-related studies and, in general, for any study requiring laboratory-generated model aerosols in the micrometre size range.

Data availability statement

The data that support the findings of this study are openly available at the following URL/DOI: <https://zenodo.org/communities/aerotox/?page=1&size=20>.

Acknowledgments

This work has received funding from the EMPIR 18HLT02 AeroTox project. The EMPIR programme is co-financed by the Participating States and from the European Union's Horizon 2020 research and innovation programme.

We thank Stefan Russi and his colleagues (Technology Sector, METAS) for technical support. We also thank Friedhelm Schneider (Grimm GmbH, Germany) for supplying the second Grimm 11-D OPSS.

ORCID iD

Konstantina Vasilatou  <https://orcid.org/0000-0002-7771-9596>

References

- European Parliament 2008 Directive 2008/50/EC of the European Parliament and of the Council of 21 May 2008 on ambient air quality and cleaner air for Europe OJ L 152, 11.6.2008 pp 1–44 (available at: <https://eur-lex.europa.eu/legal-content/en/ALL/?uri=CELEX%3A32008L0050>) (Accessed 31 August 2020)
- Fuzzi S *et al* 2015 Particulate matter, air quality and climate: lessons learned and future needs *Atmos. Chem. Phys.* **15** 8217–99
- Giordano A 2020 CFD simulation of an aerosol mixing chamber *Master Thesis* EPFL (available at: <https://infoscience.epfl.ch/record/280815>)
- Harrison R M 2020 Airborne particulate matter *Phil. Trans. R. Soc. A* **378** 20190319
- Hogrefe O, Drewnick F, Garland Lala G, Schwab J J and Demerjian K L 2004 Development, operation and applications of an aerosol generation, calibration and research facility special issue of aerosol science and technology on findings from the fine particulate matter supersites program *Aerosol Sci. Technol.* **38** 196–214
- Horender S *et al* 2021a Facility for production of ambient-like model aerosols (PALMA) in the laboratory: application in the intercomparison of automated PM monitors with the reference gravimetric method *Atmos. Meas. Tech.* **14** 1225–38
- Horender S, Auderset K and Vasilatou K 2019 Facility for calibration of optical and condensation particle counters based on a turbulent aerosol mixing tube and a reference optical particle counter *Rev. Sci. Instrum.* **90** 075111
- Horender S, Tancev G, Auderset K and Vasilatou K 2021b Traceable PM_{2.5} and PM₁₀ calibration of low-cost sensors with ambient-like aerosols generated in the laboratory *Appl. Sci.* **11** 9014
- ISO 21501-1 2009 ISO 21501-1:2009 determination of particle size distribution—single particle light interaction methods—part 1: light scattering particle spectrometer
- Kim K-H, Kabir E and Kabir S 2015 A review on the human health impact of airborne particulate matter *Environ. Int.* **74** 136–43
- Konlechner A, Goller S, Gorfer M, Molter L and Strauss J 2013 Evaluation of a calibration chamber for bioaerosol measurement devices *Gefahrstoffe Reinhaltung Luft* **73** 471–6
- Lieberherr G *et al* 2021 Assessment of real-time bioaerosol particle counters using reference chamber experiments *Atmos. Meas. Tech.* **14** 7693–706
- Liu D, Zhang Q, Jiang J and Chen D 2017 Performance calibration of low-cost and portable particular matter (PM) sensors *J. Aerosol Sci.* **112** 1–10
- Loomis D, Grosse Y, Lauby-Secretan B, El Ghissassi F, Bouvard V, Benbrahim-Tallaa L, Guha N, Baan R, Mattock H and Straif K 2013 The carcinogenicity of outdoor air pollution *Lancet Oncol.* **14** 1262–3
- Papapostolou V, Zhang H, Feenstra B J and Polidori A 2017 Development of an environmental chamber for evaluating the performance of low-cost air quality sensors under controlled conditions *Atmos. Environ.* **171** 82–90
- Pogner C *et al* 2019 A novel laminar-flow-based bioaerosol test system to determine biological sampling efficiencies of bioaerosol samplers *Aerosol Sci. Technol.* **53** 355–70
- Šauliute I *et al* 2019 Automatic pollen recognition with the Rapid-E particle counter: the first-level procedure, experience and next steps *Atmos. Meas. Tech.* **12** 3435–52
- Sauvageat E, Zeder Y, Auderset K, Calpini B, Clot B, Crouzy B, Konzelmann T, Lieberherr G, Tummon F and Vasilatou K 2020 Real-time pollen monitoring using digital holography *Atmos. Meas. Tech.* **13** 1539–50
- Schwab J J, Hogrefe O, Demerjian K L and Ambs J L 2004 Laboratory characterization of modified tapered element oscillating microbalance samplers *J. Air Waste Manage. Assoc.* **54** 1254–63
- Vasilatou K, Wälchli C, Koust S, Horender S, Iida K, Sakurai H, Schneider F, Spielvogel J, Wu T Y and Auderset K 2021 Calibration of optical particle size spectrometers against a primary standard: counting efficiency profile of the TSI model 3330 OPS and Grimm 11-D monitor in the particle size range from 300 nm to 10 μm *J. Aerosol Sci.* **157** 105818
- WHO 2013 Review of evidence on health aspects of air pollution—REVIHAAP project
- Wong L T, Chan W Y, Mui K W and Lai A C K 2010 An experimental and numerical study on deposition of bioaerosols in a scaled chamber an experimental and numerical study on deposition of bioaerosols in a scaled chamber *Aerosol Sci. Technol.* **44** 117–28